

Free-Jet Rotational Spectrum and Tunneling Motion of Difluoromethane...Xenon

Walther Caminati†

Dipartimento di Chimica "G. Ciamician" dell'Università, Via Selmi 2, I-40126 Bologna, Italy

Received: January 17, 2006; In Final Form: February 14, 2006

The rotational spectra of three isotopologues of difluoromethane...xenon have been investigated by free-jet millimeter-wave absorption spectroscopy. Only μ_c -type transitions have been observed, all of them evenly split due to the internal motion of Xe relative to the difluoromethane moiety. The vibrational splitting, 39.1(3) MHz, has been used to estimate the tunneling barrier, $V_2 = 109 \text{ cm}^{-1}$. Information on the dissociation energy has been deduced from centrifugal distortion effects ($E_B = 1.8 \text{ kJ mol}^{-1}$). The xenon atom lies in the σ_v symmetry plane of difluoromethane containing the hydrogen atoms, at an r_0 distance of 3.816 Å from its center of mass (cm), and forms a Xe–cm–C r_0 angle of 118°. The observed conformation is in agreement with the minimum found with a distributed polarizability model.

Introduction

Xenon is the most inclined of the noble gases to form chemical compounds. After the first isolation of noble gas compounds in 1962, $\text{FXe}^+\cdots\text{Pt}_2\text{F}_{11}^-$,^{1a} XeF_2 ,^{1b} and XeF_4 ,^{1c} the chemistry of xenon has grown considerably. Compounds with metal–xenon bonds² and organic molecules containing xenon atoms³ have been very recently discovered.

Vice versa, the number of identified molecular adducts of xenon with organic molecules is much smaller than those of lighter noble gases.⁴ Such a kind of molecular complex is generally investigated by rotational spectroscopy, combined with supersonic expansion techniques.^{5,6} Only a very few of these complexes, benzene–Xe,⁷ oxirane–Xe,⁸ and dimethyl ether–Xe⁹ involve, indeed, a Xe atom. This is in way surprising because, due to the higher polarizability of Xe with respect to those of lighter rare gases, a larger dispersion energy interaction is expected to stabilize complexes with Xe. However, the high mass of Xe, which makes the rotational constants of its van der Waals complexes smaller than those of the complexes of the lighter rare gases, and the high number of isotopic species, with a maximum of natural abundance (27%) for the ¹³²Xe isotope, complicate considerably the rotational spectra.

In the two above-mentioned complexes of xenon with cyclic molecules, benzene–Xe,⁷ and oxirane–Xe,⁸ the Xe atom was relatively firmly located above or below the plane of the ring, as suggested by the missing of tunneling effects. Vice versa, a small tunneling splitting (106 kHz) was observed in dimethyl ether–Xe,^{9b} which allowed for an evaluation of the potential energy surface of the Xe motions.

The adducts of difluoromethane with rare gases displayed wide tunneling splittings: 193.5 MHz for difluoromethane–Ar¹⁰ and 79.19 MHz for difluoromethane–Kr.¹¹ From these data, the potential energy surfaces have been derived.

I decided to investigate the free-jet rotational spectrum of difluoromethane–Xe ($\text{CH}_2\text{F}_2\cdots\text{Xe}$), to measure such a tunneling splitting and to estimate the potential energy surface for the Xe internal motions. Two sketches of $\text{CH}_2\text{F}_2\cdots\text{Xe}$ are given in Figure 1. The principal axis systems of CH_2F_2 and $\text{CH}_2\text{F}_2\cdots\text{Xe}$

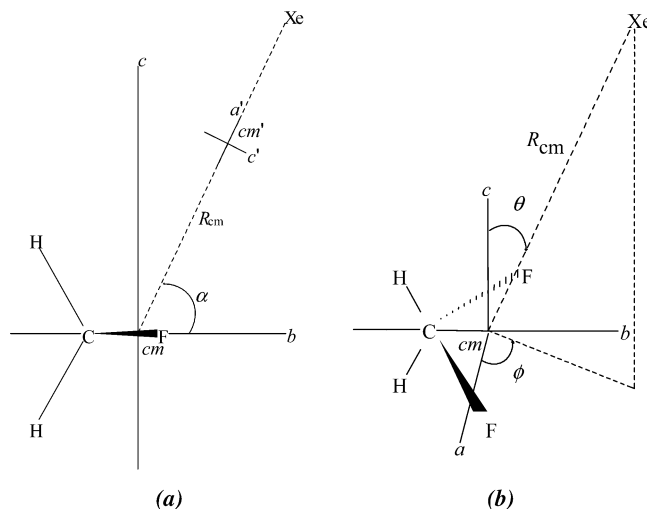


Figure 1. Sketches of $\text{CH}_2\text{F}_2\cdots\text{Xe}$ showing (a) the principal axis system of CH_2F_2 (unprimed b - and c -axes labeled) and $\text{CH}_2\text{F}_2\cdots\text{Xe}$ (primed a' - and c' -axes labeled) and the α parameter used in the flexible model analysis; the remaining axes are perpendicular to the plane of the figure; (b) the polar coordinates required for the distributed polarizability model, with the CH_2F_2 principal axis labels.

and the α parameter used in the flexible model analysis are shown in the left part (a), while the polar coordinates required for the distributed polarizability model are indicated in (b).

Experimental Methods

The Stark and pulse-modulated free-jet absorption millimeter-wave spectrometer used in this study works in the 60–78 GHz frequency region, and it has been described elsewhere.^{12,13} The accuracy of the frequency measurements is about 0.05 MHz. The complex was formed by expanding a mixture of CH_2F_2 (2%) and xenon at a pressure of ca. 1.0 bar, through a pulsed nozzle (repetition rate 5 Hz) with a diameter of 0.35 mm, to 5×10^{-3} mbar. An estimated “rotational” temperature of 5 K was attained. CH_2F_2 was supplied by Aldrich and xenon by Rivoira.

Rotational Spectrum. The rotational constants of $\text{CH}_2\text{F}_2\cdots\text{Xe}$ were estimated assuming a conformation similar

† Fax: +39 051 2099456. Phone: +39 051 2099480. E-mail: walther.caminati@unibo.it.

TABLE 1: Experimental Transition Frequencies (MHz) of CH₂F₂⋯Xe^a

$J(K_a', K_c') \leftarrow J''(K_a'', K_c'')$	¹³² Xe		¹³¹ Xe		¹²⁹ Xe	
	0 ⁻ ← 0 ⁺	0 ⁺ ← 0 ⁻	0 ⁻ ← 0 ⁺	0 ⁺ ← 0 ⁻	0 ⁻ ← 0 ⁺	0 ⁺ ← 0 ⁻
4(4)–3(3)	67822.20	67747.93	67824.27	67749.93	67828.53	67754.13
5(4)–4(3)	69577.43	69503.27	69583.43	69508.99	69594.60	69520.33
6(4)–5(3)	71330.57	71256.60	71339.80	71265.73	71358.47	71284.43
7(4)–6(3)	73081.43	73007.70	73094.13	73020.40	73120.11	73046.28
8(4)–7(3)	74829.83	74756.33	74846.00	74772.53	74879.24	74805.69
10(3,8)–9(2,8)	61034.21	60959.60	61061.38	60986.77	61117.00	61042.23
10(3,7)–9(2,7)	60929.33	60854.79	60955.60	60881.03	61009.45	60934.79
11(3,9)–10(2,9)	62798.70	62724.50	62829.52	62754.77	62892.60	62818.23
11(3,8)–10(2,8)	62642.03	62567.97	62671.53	62597.47	62732.00	62657.83

^a Transitions doubly overlapped due to near prolate degeneracy of the involved levels. Only K_a is given.

TABLE 2: Spectroscopic Constants of CH₂F₂⋯Xe (S Reduction, I^r Representation)

	¹³² Xe		¹³¹ Xe		¹²⁹ Xe	
	0 ⁺	0 ⁻	0 ⁺	0 ⁻	0 ⁺	0 ⁻
A/MHz	9560.75(2) ^a	9560.60(2)	9560.84(2)	9560.67(2)	9560.91(2)	9560.75(2)
B/MHz	913.02(3)	913.00(3)	915.00(3)	914.94(3)	918.86(3)	918.84(3)
C/MHz	851.79(3)	851.80(3)	853.52(3)	853.55(3)	856.88(3)	856.89(3)
D_J/kHz^b		4.29(8)		4.45(8)		4.36(8)
D_{JK}/kHz		98.7(4)		99.7(4)		99.8(4)
$\Delta E/\text{MHz}$		39.1(3)		39.4(3)		39.3(3)
N^c		18		18		18
σ/MHz^d		0.09		0.13		0.09

^a The quantity in parentheses is the standard error in units of the last digit of the quoted value. ^b The remaining quartic centrifugal distortion parameters have been fixed to zero because they were undetermined in the fit. ^c Number of transitions in the fit. ^d Standard deviation of the fit.

to that of CH₂F₂⋯Ar¹⁰ and CH₂F₂⋯Kr,¹¹ that is with the xenon atom lying in the HCH plane and forming a Xe–cm–C angle of ca. 120° (see Figure 1). A trial starting value of 3.8 Å was assumed for the distance of Xe from the center of mass (cm) of CH₂F₂. The r_0 geometry of CH₂F₂¹⁴ has been assumed to be unaltered in the complex. As usual for such a kind of complex, there is a switch of axes in going from the molecule to the adduct so that the μ_b -type spectrum of CH₂F₂ is converted to a predominantly μ_c -type spectrum in the complex. Also the μ_a dipole moment component is not zero so that rotational lines involving asymmetry near-degenerate levels are easily Stark modulated.

The rotational spectra of the three most abundant isotopic species, with ¹³²Xe, ¹²⁹Xe, and ¹³¹Xe (≈27%, ≈26%, and ≈21% natural abundance, respectively), were investigated. Nine μ_c -type transitions have been measured for each isotopologue. All of them were split into two component lines separated by ca. 74 MHz, showing unequivocally that a tunneling motion which inverts the μ_c dipole moment component through a low barrier takes place in the complex. A 10/6 statistical weight was observed for all lines, depending on the parity of K_a and ν . This effect is discussed below. No μ_a -type transitions have been observed: they would involve energy levels with too high J numbers to be populated at 5 K.

The experimental frequencies, listed in Table 1, were fitted with a Pickett-type coupled Hamiltonian:^{15,16}

$$H = H_R(0^+) + H_R(0^-) + H_{CD} + \Delta E \quad (1)$$

with $H_R(0^+)$ and $H_R(0^-)$ representing the rigid rotational parts of the Hamiltonian for the 0⁺ and 0⁻ states, respectively. ΔE is the vibrational spacing between the two states. The centrifugal distortion contributions (S reduction and I^r representation)¹⁷ are represented by H_{CD} and were assumed to be the same in both states. The obtained spectroscopic constants are shown for all isotopomers in Table 2, together with some statistical parameters of the fits.

Statistical Weight. In the following we will consider the observed splitting to be produced by only one of the two possible internal rotations of CH₂F₂. This hypothesis, which is interpreted by the model calculations of the following sections, is also supported by the statistical weight of 10/6 mentioned above and is in favor of even K_a values for transitions starting from $\nu = 0$ and in favor of odd K_a values for transitions starting from $\nu = 1$. This means that the barrier to the Xe tunneling is quite low and that the complex possesses a quantomechanical C_{2v} symmetry. Looking to Figure 1, we have to think that Xe is delocalized above and below the F–C–F plane. Then, the effective a inertial axis is of a C_2 the molecular symmetry axis. CH₂F₂⋯Xe contains, with respect to this axis, two pairs of equivalent fermions (two equivalent hydrogens and two equivalent fluorines) and follows the Bose–Einstein statistics, i.e., the overall wave function

$$\psi_{\text{tot}} = \psi_e \psi_\nu \psi_R \psi_s \quad (2)$$

must be symmetric. The electronic wave function ψ_e is symmetric in the ground state; the vibrational wave function ψ_ν is symmetric for the 0⁺ and antisymmetric for the 0⁻ states, respectively. The spin function ψ_s (10 A_g; 6 A_u) does have a ratio of 5/3 between symmetric and antisymmetric components. Then, for 0⁺, the rotational transitions with a symmetric initial state ψ_R will have a favorable intensity ratio of 5/3, with respect to the antisymmetric ones; the opposite is true for the 0⁻ state. With the C_2 symmetry axis lying along the a -axis, the even rotational functions are characterized by an even value of K_a , and vice versa. The observed intensity variations are consistent with the 5/3 intensity ratio.

Location of the Xenon Atom in the Complex. The r_s coordinates¹⁸ of the xenon atom can be obtained in the principal axes system of CH₂F₂ by a hypothetical substitution of an atom of zero mass with a Xe in going from CH₂F₂ to CH₂F₂⋯Xe, or in the principal axes system of CH₂F₂⋯¹³²Xe when substituting ¹³²Xe with ¹²⁹Xe. The two sets of data are shown in Table 3.

TABLE 3: r_s Coordinates of Xe in the Principal Axis Systems of CH_2F_2 and $\text{CH}_2\text{F}_2\cdots\text{Xe}$

	CH_2F_2	$\text{CH}_2\text{F}_2\cdots\text{Xe}$
$ a /\text{\AA}$	0.320(7)	1.075(3)
$ b /\text{\AA}$	2.091(7)	0.03(9)
$ c /\text{\AA}$	3.210(4)	0.03(11)

TABLE 4: r_s and r_0 and r_{DPM} Structural van der Waals Parameters (see Text and Figure 1)

	r_s^a	r_0^a	r_{DPM}
$R_{\text{cm}}/\text{\AA}$	3.817(5)	3.816 (8)	3.754
θ/deg	33.1	27.7(2)	26.3

^a The Xe atom was constrained in the HCH plane.

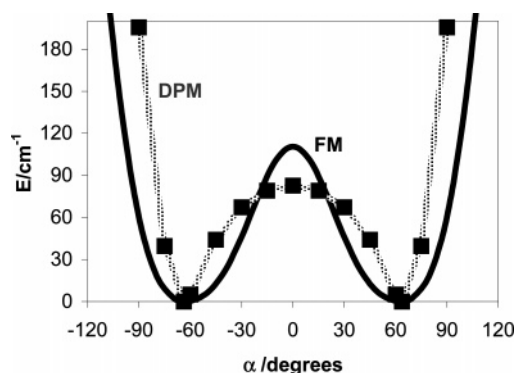
**Figure 2.** Picture of the complex, according to the r_0 structure.

The small, but quite larger than the error, value of $|a|$ for the first case can be due to the Coriolis effects of large amplitude van der Waals vibrations.¹⁹ Alternatively, it can be attributed to a larger uncertainty on the rotational constants than that reported in Table 2, because of their correlation with the F_{ac} Coriolis coupling parameter. This parameter, indeed, is not determined due to the small number of available transitions. The r_s coordinates in the principal axes system of the complex are more reliable, because the vibrational contributions in the two isotopologues are practically the same.

In Table 4 we report a partial r_0 structure of the complex, obtained fitting the distance R_{cm} and the angle θ (see Figure 1) to the available rotational constants. The geometry of difluoromethane has been fixed to that of the isolated molecule,¹⁴ and xenon has been assumed to lie in the HCH plane. There we report also the r_s values of these two parameters, obtained from the substitution coordinates of Table 3. Finally, the values calculated by a distributed polarizability model (see the following sections) are given. The complex is shown in Figure 2, according to the r_0 structure.

van der Waals Vibrations. The motions of the rare gas atom (RG) in a molecular complex are generally described by a radial part, the stretching of RG with respect to the cm of the partner molecule, and an angular part, which can be thought of as two bending motions described by θ and ϕ (Figure 1b) of Xe in the complex. We will discuss below how the potential energy surface of these motions can be interpreted with a simple electrostatic model, how the observed splitting can be used to scale the theoretical potential energy surface, and how to estimate the dissociation energy from centrifugal distortion effects.

a. Distributed Polarizability Model. The distributed polarizability model (DPM) has proved to be an economic but efficient method to find the different possible minima on the van der Waals potential energy surface.^{20,21} We ran DPM calculations by using the computer program RGDMIN.²² The geometry of CH_2F_2 was fixed to the r_0 structure,¹⁴ and the distance (R_{cm}) between its cm and the RG was optimized in the full range of θ and ϕ , with steps $\Delta\phi = \Delta\theta = 15^\circ$, being that R_{cm} , θ , and ϕ

**Figure 3.** Lowest energy tunneling pathways (described by the α of Figure 1) as obtained by the DPM model (grey line) and the flexible model calculations (FM, black line).

are the spherical coordinates shown in Figure 1b. The obtained potential energy surface has minima at $\phi = 90^\circ$ and $\theta = 26.3$ and 153.7° , similar to that given in Figure 3 of the article on $\text{CH}_2\text{F}_2\cdots\text{Kr}$.¹¹ The minimum energy tunneling pathway between the two equivalent minima occurs through a barrier at a C_{2v} configuration of the adduct in which the Xe atom is coplanar with the FCF fragment of CH_2F_2 . It can be described by the angle α of Figure 1a, in the range of $-120^\circ < \alpha < 120^\circ$. The corresponding DPM potential energy function is given (grey curve, dots) in Figure 3.

b. Tunneling Motion Described by One-Dimensional Flexible Model Calculations. If the pathways assumed above are responsible for the observed μ_c -type tunneling splittings, we can use the splitting to scale the DPM barrier. Meyers's one-dimensional flexible model²³ can be used for this purpose. To apply it, we have to model the DPM potential energy function with an analytical function. The DPM maxima and minima found along the pathway can be reproduced with the following function:

$$V(\alpha)/\text{cm}^{-1} = 213.6(\cos \alpha - \cos \alpha_0)^2(1 + 0.35 \cos 3\alpha) \quad (3)$$

where α_0 ($= 63.6^\circ$) is the value of α at the global minimum. Although α is related to θ (through a shift of 90° or 270° , depending on ϕ , see Figure 1), we needed to use α within this model, because it is defined in the full 2π range, while θ is defined only in the $0-180^\circ$ range. The factor $(\cos \alpha - \cos \alpha_0)^2$ of eq 3 fixes the position of the two equivalent minima at α_0 , while the second one defines the positions and the relative values of the other stationary points. Equation 3 is valid only in the range of $\pm 100^\circ$, since the pathways becomes bifurcated at higher values of α , similarly to what shown in Figure 3 of ref 11.

A large structural relaxation was found for R_{cm} as a function of α , which can be parametrized as

$$R_{\text{cm}}(\alpha)/\text{\AA} = R_0 + \Delta R(\cos \alpha - \cos \alpha_0)^2(1 + 0.35 \cos 3\alpha) \quad (4)$$

The values $R_0 = 3.816$ and $\Delta R = 0.323 \text{ \AA}$, suggested by the DPM model, have been used.

The experimental splitting has been reproduced when scaling eq 3 by a factor 1.325. Correspondingly, the inversion barrier, compared in Table 3 to that of $\text{CH}_2\text{F}_2\cdots\text{Ar}$ and $\text{CH}_2\text{F}_2\cdots\text{Kr}$, was 109 cm^{-1} , for which we can estimate a 10% error, related to the uncertainty of the shape of the potential energy function. The profile of scaled $V(\alpha)$ is given by the black line of Figure 3.

TABLE 5: R_{cm} , Dissociation Energy, and Barrier to Inversion for $\text{CH}_2\text{F}_2\cdots\text{RG}$, with $\text{RG} = \text{Ar}$, Kr , and Xe

	$\text{CH}_2\text{F}_2\cdots\text{Ar}^a$	$\text{CH}_2\text{F}_2\cdots\text{Kr}^b$	$\text{CH}_2\text{F}_2\cdots\text{Xe}$
$R_{\text{cm}}/\text{\AA}$	3.35	3.616	3.816
$E_{\text{B}}/\text{kJ mol}^{-1}$	1.5	1.9	1.8
$V_{\text{inv}}/\text{kJ mol}^{-1}$	1.20(5)	1.23(5)	1.31(5)

^a Ref 10. ^b Ref 11.

In the flexible model calculations the α coordinate has been considered in the $\pm 115^\circ$ range and solved into 57 mesh points.²³

c. van der Waals Stretching. For asymmetric top complexes, in which the stretching coordinate is near-parallel to the inertial a -axis, the stretching force constant (k_s) can be estimated by approximating the complex to a molecule made of two rigid parts and using equations of the following type:^{24,25}

$$k_s = 16\pi^4 \mu^2 R_{\text{cm}}^2 [4B^4 + 4C^4 - (B - C)^2(B + C)^2] / (hD_J) \quad (5)$$

The B , C , and D_J are the spectroscopic constants of the molecular complex, μ is the pseudodiatomic reduced mass, and R_{cm} is the distance between the centers of mass of the monomers. Using the r_0 value $R_{\text{cm}} = 3.816 \text{ \AA}$ we obtained $k_s = 1.49 \text{ N}\cdot\text{m}^{-1}$, corresponding to a harmonic stretching fundamental, $\nu_s = 26 \text{ cm}^{-1}$.

A Lennard-Jones potential is generally assumed for the stretching potential energy function. It is then possible to estimate the dissociation energy, $E_{\text{B}} = 1.82 \text{ kJ mol}^{-1}$ in our case, using the approximated equation:²⁶

$$E_{\text{B}} = k_s R_{\text{cm}}^2 / 72 \quad (6)$$

These values are compared to those of the related complex $\text{CH}_2\text{F}_2\cdots\text{Ar}$ and $\text{CH}_2\text{F}_2\cdots\text{Kr}$ in Table 5. It is difficult to estimate the error on this kind of data, depending, apart the pseudodiatomic approximation, on the contributions to D_J from other vibrations besides the van der Waals stretching. It is, however, assumed to be within 10–20% of the value itself.

Conclusions

The rotational spectra of three isotopologues of the complex $\text{CH}_2\text{F}_2\cdots\text{Xe}$ display splittings, 39.2(3) MHz, that are the same within experimental error and are due to the internal rotation of CH_2F_2 . Up to this point in time, this is the largest tunneling splitting observed for a complex of Xe with an organic molecule. From this splitting an estimate of the potential energy surface has been made. The agreement with the results obtained with a simple distributed polarizability model is quite good.

The dissociation energy and the barrier to the tunneling are similar to those of the homologue complexes $\text{CH}_2\text{F}_2\cdots\text{Ar}^{10}$ and

$\text{CH}_2\text{F}_2\cdots\text{Kr}^{11}$. The higher tunneling splittings for these two complexes are attributable to their lower reduced masses.

The features of the rotational spectrum of the lighter member of the series, $\text{CH}_2\text{F}_2\cdots\text{Ne}$, are completely different. Its rotational spectrum has been observed and assigned, but it is much more complicated and not yet fully understood.²⁷ This is presumably due to a combination of a much smaller reduced mass of the Ne motions and to a flatter potential energy surface.

Acknowledgment. The author thanks Aldo Millemaggi for technical help. This work was supported by the University of Bologna and the Ministero dell'Università e della Ricerca Scientifica e Tecnologica.

References and Notes

- (1) (a) Bartlett, N. *Proc. Chem. Soc.* **1962**, 218. (b) Hoppe, R.; Dähne, W.; Mattauch, H.; Rodder, K. M. *Angew. Chem.* **1962**, *74*, 903; *Angew. Chem., Int. Ed. Engl.* **1962**, *1*, 599. (c) Claasen, H.; Selig, H. J.; Malm, G. *J. Am. Chem. Soc.* **1962**, *84*, 3593.
- (2) (a) Hwang, I.-C.; Seidel, S.; Seppelt, K. *Angew. Chem., Int. Ed.* **2003**, *42*, 4392. (b) Seppelt, K. *Z. Anorg. Allg. Chem.* **2003**, 629, 2427.
- (3) Frohn, H.-J.; Theissen, M. *J. Fluorine Chem.* **2004**, *125*, 981.
- (4) Novick, S. E. *Bibliography of Rotational Spectra of Weakly Bound Complexes*; 2005; available at <http://www.wesleyan.edu/chem/bios/vd-w.html>.
- (5) Anderson, J. B.; Andres, R. P.; Fenn, J. B. In *Advances in Chemical Physics*; Ross, J., Ed.; Interscience: New York, 1966; Vol. X, pp 275–317.
- (6) Scoles, G., Ed. *Atomic and Molecular Beam Methods*; Oxford University Press: New York, 1992; Vols. I, II.
- (7) Brupbacher, Th.; Makarewicz, J.; Bauder, A. *J. Chem. Phys.* **1994**, *101*, 9736–9746.
- (8) Velino, B.; Favero, P. G.; Caminati, W. *J. Chem. Phys.* **2002**, *117*, 5688–5691.
- (9) (a) Favero, L. B.; Velino, B.; Millemaggi, A.; Caminati, W. *ChemPhysChem* **2003**, *4*, 881–884. (b) Caminati, W.; Millemaggi, A.; Alonso, J. L.; Lesarri, A.; López, J. C.; Mata, S. *Chem. Phys. Lett.* **2004**, *392*, 1–6.
- (10) López, J. C.; Favero, P. G.; Dell'Erba, A.; Caminati, W. *Chem. Phys. Lett.* **2000**, *316*, 81.
- (11) Maris, A.; Melandri, S.; Caminati, W.; Rossi, I. *Chem. Phys. Lett.* **2005**, *407*, 192–198.
- (12) Melandri, S.; Maccaferri, G.; Maris, A.; Millemaggi, A.; Caminati, W.; Favero, P. G. *Chem. Phys. Lett.* **1996**, *261*, 267–271.
- (13) Melandri, S.; Caminati, W.; Favero, L. B.; Millemaggi, A.; Favero, P. G. *J. Mol. Struct.* **1995**, *352/353*, 253–258.
- (14) (a) Hirota, E. *J. Mol. Spectrosc.* **1978**, *71*, 145–159. (b) Lide, D. R., Jr. *J. Am. Chem. Soc.* **1952**, *74*, 3548–3552.
- (15) Pickett, H. M. *J. Chem. Phys.* **1972**, *56*, 1715–1723.
- (16) Pickett, H. M. *J. Mol. Spectrosc.* **1991**, *148*, 371–377.
- (17) Watson, J. K. G. In *Vibrational Spectra and Structure*; Durig, J. R., Ed.; Elsevier: Amsterdam, 1977; Vol. 6, pp 1–89.
- (18) Kraitchman, J. *Am. J. Phys.* **1953**, *21*, 17–25.
- (19) Caminati, W.; Favero, P. G.; Melandri, S.; Meyer, R. *Chem. Phys. Lett.* **1997**, *268*, 393–400.
- (20) Kisiel, Z. *J. Phys. Chem.* **1991**, *95*, 7605.
- (21) Kisiel, Z.; Fowler, P. W.; Legon, A. C. *J. Chem. Phys.* **1991**, *95*, 2283.
- (22) Kisiel, Z. *PROSPE—Programs for Rotational SPEctroscopy*; available at <http://info.ifpan.edu.pl/~kisiel/prospe.htm>.
- (23) Meyer, R. *J. Mol. Spectrosc.* **1979**, *76*, 266–300.
- (24) Millen, D. J. *Can. J. Chem.* **1985**, *63*, 1477–1479.
- (25) Read, W. G.; Campbell, E. J.; Hederson, J. J. *J. Chem. Phys.* **1983**, *78*, 3501–3508.
- (26) Bettens, R. P. A.; Spycher, R. M.; Bauder, A. *Mol. Phys.* **1995**, *86*, 487–511.
- (27) Caminati, W.; et al. Presented at the 16th Colloquium on High-Resolution Molecular Spectroscopy, Dijon, France, Sept 6–10, 1999; Invited Lecture P2.